Eur Radiol (2007) 17: 1663–1668
DOI 10.1007/s00330-006-0558-x

S. Rodrigo
C. Oppenheim
F. Chassoux
N. Golestani
Y. Cointepas
C. Poupon
F. Semah
J.-F. Mangin
D. Le Bihan
J.-F. Meder

Uncinate fasciculus fiber tracking in mesial temporal lobe epilepsy. Initial findings

Received: 8 July 2006
Revised: 24 November 2006
Accepted: 1 December 2006
Published online: 12 January 2007

S. Rodrigo · C. Oppenheim (✉) · J.-F. Meder
Département d'Imagerie Morphologique et Fonctionnelle,
Université Paris-Descartes,
Faculté de Médecine,
Centre Hospitalier Sainte-Anne,
75674 Paris, France
e-mail: c.oppenheim@ch-sainte-anne.fr
Tel.: +33-1-45658242
Fax: +33-1-45658073

F. Chassoux
Université Paris-Descartes, Faculté de Médecine, Service de Neurochirurgie,
Centre Hospitalier Sainte-Anne,
75674 Paris, France

N. Golestani · Y. Cointepas · C. Poupon · F. Semah · J.-F. Mangin · D. Le Bihan
Service Hospitalier Frédéric Joliot,
CEA,
91401 Orsay cedex, France

Abstract In temporal lobe epilepsy (TLE) due to hippocampal sclerosis (HS), ictal discharge spread to the frontal and insulo-perisylvian cortex is commonly observed. The implication of white matter pathways in this propagation has not been investigated. We compared diffusion tensor imaging (DTI) measurements along the uncinate fasciculus (UF), a major tract connecting the frontal and temporal lobes, in patients and controls. Ten right-handed patients referred for intractable TLE due to a right HS were investigated on a 1.5-T MR scanner including a DTI sequence. All patients had interictal fluorodeoxyglucose PET showing an ipsilateral temporal hypometabolism associated with insular and frontal or perisylvian hypometabolism. The controls consisted of ten right-handed healthy subjects. UF fiber tracking was performed, and its fractional anisotropy (FA) values were compared between patients and controls, separately for the right and left UF. The left-minus-right FA UF asymmetry index was computed to test for intergroup differences. Asymmetries were found in the control group with right-greater-than-left FA. This asymmetrical pattern was lost in the patient group. Right FA values were lower in patients with right HS versus controls. Although preliminary, these findings may be related to the preferential pathway of seizure spread from the mesial temporal lobe to frontal and insulo-perisylvian areas.

Keywords Mesial temporal lobe epilepsy · Hippocampal sclerosis · Diffusion tensor imaging · Fiber tracking

Introduction

Characterization of epilepsy remains a challenging issue in the field of neuroimaging. Conventional magnetic resonance (MR) pulse sequences, such as T1- and T2-weighted and diffusion imaging, are needed to find the epileptogenic zone accurately [1]. Diffusion tensor imaging (DTI) is a noninvasive magnetic resonance (MR) imaging technique that can be used to quantify the diffusion properties of brain tissues [2, 3]. A tissue is said to be isotropic when diffusion is identical in all directions. Conversely, it is considered to be anisotropic when water molecules move in a preferential direction. White matter (WM) is a highly anisotropic structure, presumably due to the fact that water molecules move along the main axis of myelinated fibers. A disruption of this microstructural environment will lead to a less orderly arrangement of nerve fibers and subsequent changes in anisotropy [3]. A few studies have

addressed the usefulness of DTI in patients with intractable epilepsy and have demonstrated increased diffusivity and reduced anisotropy in cerebral areas corresponding to the epileptogenic focus [4, 5]. Others have reported that white matter changes were not only restricted to the lesion seen on conventional MR sequences, but extended into other brain regions distant from the lesion [6, 7]. The fact that lesions are more widespread than can be seen on conventional T2-weighted MR sequences has already been demonstrated by structural imaging data in patients with hippocampal sclerosis (HS) [8, 9]. Metabolic studies have also demonstrated that the zone of hypometabolism observed in temporal lobe epilepsy (TLE) is usually much larger than the structural lesion and epileptogenic zone [10, 11], often spreading over extra-temporal cortical areas [12–14]. More recently, temporo-fronto-insulo-perisylvian hypometabolism was shown to be the usual pattern in patients with HS [15]. These findings are consistent with electrophysiological and previous metabolic data reported in TLE [16–18] and could be related to the pathways in which ictal discharge spreads in extra-temporal areas. The uncinate fasciculus (UF) is a major fiber tract connecting the inferior frontal and anterior temporal lobes [19]. We hypothesized that this tract may be involved in ictal discharge spread along white matter fiber bundles. We used quantitative DTI measurements along the segmented UF bundle in patients with mesial TLE associated with HS and compared these to similar measures obtained in healthy controls. We predicted microstructural differences to be more prominent in the UF ipsilateral to the HS between groups.

Materials and methods

Subjects

The patient group consisted of ten right-handed patients (five males and five females) aged from 16 to 42 years (median: 31 years), referred for refractory TLE associated with a right HS. This diagnosis relied on electro-clinical data, video-EEG recordings and MR imaging. In addition, all patients underwent an interictal [^{18}F] fluorodeoxyglucose positron emission tomography (PET) scan showing an ipsilateral temporal hypometabolism associated with insular involvement and frontal or perisylvian hypometabolism.

The control group consisted of ten right-handed healthy subjects (six males and four females, aged from 20 to 33 years, median: 23 years). All patients and control subjects gave their written informed consent to participate in the study, which was approved by the local ethical committee.

Image acquisition and analysis

All patients and controls were investigated on a 1.5-T Signa MR scanner (GE Medical Systems, Milwaukee, WI), including a T_1-weighted three-dimensional spoiled-gradient-recalled and a high-resolution DTI sequence using the following parameters: 41 diffusion gradient directions (b value of 700 s/mm^2) as well as 5 images without diffusion weighting, 24 cm FOV, 128×128 acquisition matrix, 60 slices and z resolution of 2.0 mm. DTI data were transferred to an independent workstation and analyzed using "Brainvisa/Anatomist" software [20]. After correction for eddy current distortions [21], the diffusion tensor [3] and parametric maps, including fractional anisotropy (FA) and color maps [22], were computed. UF segmentation was performed using a fiber-tracking algorithm ("Brainvisa/Anatomist" software), as proposed by Conturo et al. [23]. The UF is a long association white matter bundle that connects the anterior portion of the temporal lobe with the orbital frontal gyrus (Fig. 1). It arises from the temporal lobe lateral to the amygdala and hippocampus, courses through the temporal stem and has a characteristic hooked shape as it curves upward into the extreme and external capsule to continue into the orbital gyrus [24]. The following steps were applied to each UF bundle, bilaterally: (1) temporal region of interest (ROI) positioning: on a coronal reformatted color map, we first identified the temporal hook of the UF, i.e., a temporo-mesial structure located below the anterior commissura with a main direction in the z-axis. The ROI (mean: 16 pixels) was then placed on the hook of the UF on the axial color map; (2) single-ROI tractography: the FACT (fiber assignment by continuous tracking) algorithm [25] was used with an angular threshold >45° and keeping only voxels with FA >0.2 to restrict fiber assignment to white matter, using 32 seed points per voxel. This allowed us to delineate three components arising from the temporal stem and projecting to the anterior part of the temporal lobe, to the orbital frontal gyrus and to the occipital lobe. These fibers corresponded to two major bundles, namely the UF (temporo-frontal) and the inferior fronto-occipital fasciculus; (3) frontal ROI positioning: a fronto-basal ROI (mean: 81 pixels) was placed anteriorly to the genu of the corpus callosum on the coronal view; (4) two-ROI tractography: only fibers that crossed both ROIs were retained (Fig. 2) so as to separate the UF from the inferior fronto-occipital fasciculus and avoid picking up the latter. UF tracking was considered complete when continuous pixels connected the temporal region to the orbital frontal gyrus. FA values were compared between patients and controls, separately for the right and left UF. The FA UF left-minus-right asymmetry index was computed within each group to test for intergroup differences. All comparisons were done using a non-parametric Wilcoxon signed rank test for paired data and a Wilcoxon rank sum test for unpaired data. Statistics were computed using the R stats package [26], and $P<0.05$ was considered significant.

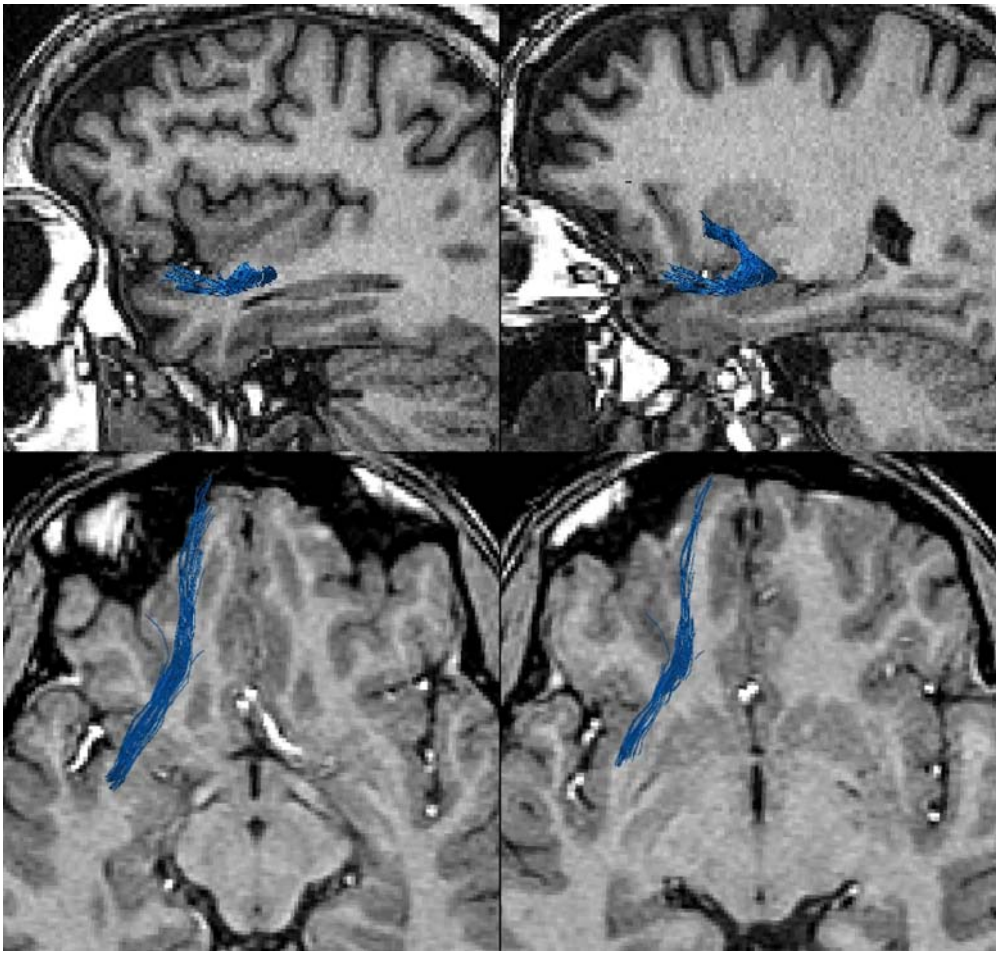

Fig. 1 Right uncinate fasciculus fiber tracking projected on T1-weighted MR views. Upper left: temporal part of the bundle curving toward the insula; upper right: the hooked shape insular part; lower left: the end of the hooked shape as it curves upward; lower right: frontal extremity of the uncinate fasciculus

Results

The control and patient groups did not differ significantly for age and sex ratio. The UF fiber tracking was complete in all the subjects. Illustrative examples of UF tracking in patient and the control groups are presented in Figs. 3 and 4. There was a significant side-to-side asymmetry in FA values in the control group (P=0.04), but not in the patient group (Fig. 5). Intergroup comparisons showed the following: the right FA values were significantly lower in the patient (mean ± SD=0.43±0.05) compared to the control group (0.48±0.02) (P=0.005). The mean left FA values were not significantly different between the patient (0.45±0.03) compared to the control group (0.45±0.02). The FA index (left minus right) was significantly different between groups (P=0.009), being negative in the control group (−0.02±0.02) and positive in the patient group (0.01±0.03).

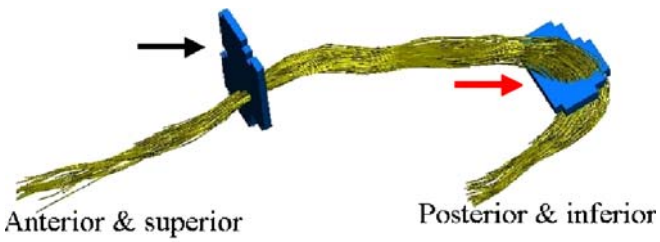

Fig. 2 Uncinate fasciculus fiber tracking-fibers that pertained to both regions of interest (ROIs) were retained (frontal ROI: black arrow; temporal stem ROI: red arrow)

Discussion

We found decreased anisotropy in the right UF in temporal lobe epilepsy associated with right HS. This result was obtained by measuring the mean FA within the UF, identified by the use of a two-ROI fiber-tracking algorithm. The significance of this finding will be discussed taking into account the pathway of seizure spread from mesial temporal structures to extra-temporal areas.

Control group

The mean FA values measured along the right and left UF (0.48 and 0.45, respectively) were higher than previously

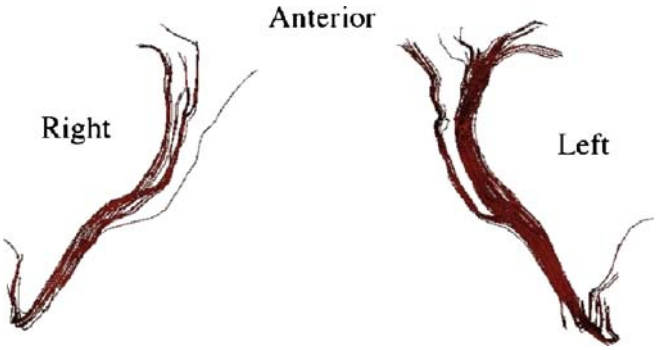

Fig. 3 Illustrative example of uncinate fasciculus tracking in the patient group

reported normative values [27]. This discrepancy may have resulted from methodological differences between our study and previous ones. We chose a high angular echo planar DTI (41 directions) and contiguous 2.0-mm-thick sections, while for example, Kubicki and colleagues (2002) used line-scan DTI with 6 diffusion directions and a slice thickness of 4 mm plus 1 mm interslice gap [27]. Due to these methodological differences, our values are likely to have been less contaminated by partial volume effects. We measured the FA along both frontal and temporal UF portions, whereas previously reported values were computed at the level of the UF temporal stem [27]. Our values are thus more representative of the whole UF. In right-handed controls, we found a significant right-greater-than-left asymmetry in UF FA values. Although the asymmetry of the UF in controls is still controversial [27, 28], our results are consistent with previous imaging findings using voxel-by-voxel DTI analysis, which showed a right-greater-than-left FA asymmetry in the stem and the inferior aspect of the UF [28]. Furthermore, a postmortem study has shown that the right UF is larger and contains more fibers than the left UF, suggesting greater right-sided

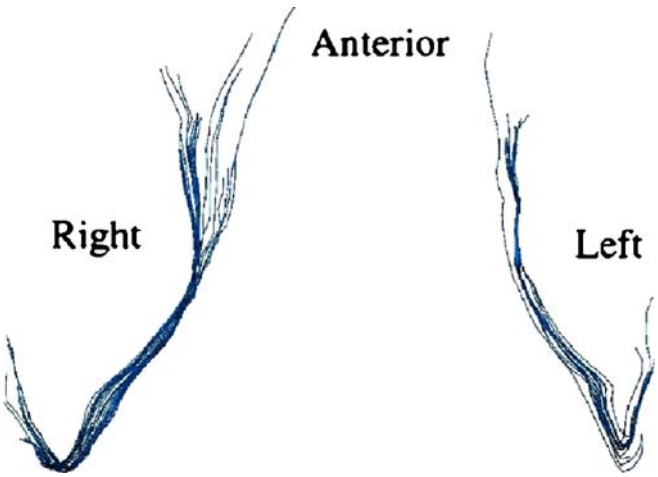

Fig. 4 Illustrative example of uncinate fasciculus tracking in the control group

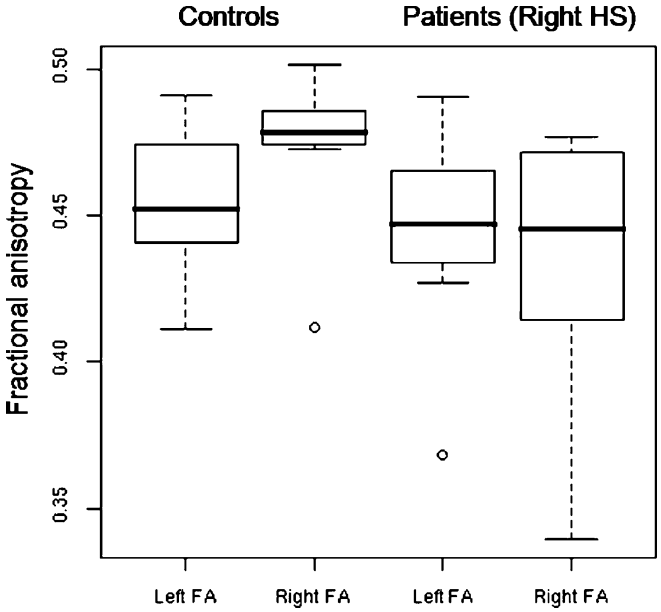

Fig. 5 Boxplot of fractional anisotropy in controls and patients with right hippocampal scelrosis (HS). Each box has a line at the first quartile, median and third quartile values. The whiskers are lines extending from each end of the box to show the extent of the rest of the data. Outliers (○) are data with values beyond the ends of the whiskers

fronto-temporal connectivity in healthy adult human brains [29]. Although the right-greater-than-left UF asymmetry did not depend on gender in the latter postmortem study, we chose to match controls and patients for gender since DTI has shown that this parameter influences microstructure in several human brain regions [30]. For similar reasons, we selected right-handed patients and controls and minimized age differences between groups to avoid potential confounds of handedness and age [31–33].

HS patient group

We expected microstructural differences between the patient and control group to be more prominent in the UF ipsilateral to the HS. In line with this hypothesis, we found a significantly lower anisotropy in the right UF in patients with TLE associated with right HS when compared to controls. This could explain why patients lacked right-greater-than-left FA asymmetry, which we observed in controls. Previous findings have suggested that anisotropy changes in patients with chronic epilepsy encompass the structural lesion and involve areas that appear normal on conventional MR images [6, 7, 34]. DTI changes have been detected in structures outside the temporal lobe, such as the external capsule, the posterior corpus callosum and the extratemporal limbic lobe in TLE [6, 35]. Although previous TLE pathological studies reported bilateral involvement of limbic structures, especially the hippocam-

pal formations [36, 37], we did not find any significant FA changes controlateral to the HS side. This, however, does not rule out subtle microstructural changes that may be associated with the contralateral spread of the ictal discharge that originates from the epileptogenic temporal lobe. To search for widespread microstructural changes, an alternative would have been to investigate the whole dataset using voxel-by-voxel analysis [28, 38]. Based on the metabolic and electrical patterns in this patient population, however, we chose not to use this method, but rather to focus on the UF, driven by our initial hypothesis.

Pathophysiological implications

Several mechanisms might explain the lack of FA asymmetry, as well as the preferential FA reduction in the right UF, ipsilateral to the HS in TLE patients. These changes might reflect a deficit in myelin or less tightly packed neuronal networks. Gliosis or microdysgenesis, which are frequently associated with HS in patients with intractable TLE [39, 40], could account for the loss of white matter integrity. Wallerian degeneration secondary to chronic epilepsy and neuronal loss has also been suggested [31]. The role of the UF in the spread of seizures originating from mesial temporal structures is suggested by anatomical, electrophysiological and metabolic data [15, 19, 41]. Our DTI results, obtained in patients with a large temporo-fronto-insulo-perisylvian PET hypometabolism, could support the implication of the UF in the ictal network. Further studies are needed to validate the hypothesis that the decrease of anisotropy in white matter bundles results from repeated ictal spread. In this regard, longitudinal DTI studies including patients that do not require surgery could help testing this hypothesis. Beside the uncinate fasciculus, other white matter bundles should be studied, and DTI measurements should be compared between subgroups of TLE patients with different metabolic and electro-clinical patterns [15].

Conclusion

We found a right-greater-than-left asymmetry in FA along the uncinate fasciculus in normal subjects, whereas this asymmetry was no longer observed in TLE patients with right HS. These findings may suggest the implication of the UF in the ictal discharge spread over extra-temporal areas, especially towards the frontal lobe in these patients. In the future, DTI may represent a useful adjunct to PET for improving our understanding of the ictal spread network in TLE.

References

1. Urbach H (2005) Imaging of the epilepsies. Eur Radiol 15:494–500
2. Le Bihan D et al (2001) Diffusion tensor imaging: concepts and applications. J Magn Reson Imaging 13:534–546
3. Pierpaoli C, Jezzard P, Basser PJ, Barnett A, Di Chiro G (1996) Diffusion tensor MR imaging of the human brain. Radiology 201:637–648
4. Assaf BA et al (2003) Diffusion tensor imaging of the hippocampal formation in temporal lobe epilepsy. AJNR Am J Neuroradiol 24:1857–1862
5. Wieshmann UC, Clark CA, Symms MR, Barker GJ, Birnie KD, Shorvon SD (1999) Water diffusion in the human hippocampus in epilepsy. Magn Reson Imaging 17:29–36
6. Arfanakis K, Hermann BP, Rogers BP, Carew JD, Seidenberg M, Meyerand ME (2002) Diffusion tensor MRI in temporal lobe epilepsy. Magn Reson Imaging 20:511–519
7. Dumas de la Roque A et al (2005) Diffusion tensor imaging of partial intractable epilepsy. Eur Radiol 15:279–285
8. Moran NF, Lemieux L, Kitchen ND, Fish DR, Shorvon SD (2001) Extrahippocampal temporal lobe atrophy in temporal lobe epilepsy and mesial temporal sclerosis. Brain 124:167–175
9. Sisodiya SM et al (1997) Correlation of widespread preoperative magnetic resonance imaging changes with unsuccessful surgery for hippocampal sclerosis. Ann Neurol 41:490–496
10. Henry TR, Mazziotta JC, Engel J Jr (1993) Interictal metabolic anatomy of mesial temporal lobe epilepsy. Arch Neurol 50:582–589
11. Theodore WH, Sato S, Kufta C, Balish MB, Bromfield EB, Leiderman DB (1992) Temporal lobectomy for uncontrolled seizures: the role of positron emission tomography. Ann Neurol 32:789–794
12. Arnold S et al (1996) Topography of interictal glucose hypometabolism in unilateral mesiotemporal epilepsy. Neurology 46:1422–1430
13. Dupont S, Semah F, Baulac M, Samson Y (1998) The underlying pathophysiology of ictal dystonia in temporal lobe epilepsy: an FDG-PET study. Neurology 51:1289–1292
14. Savic I, Altshuler L, Baxter L, Engel J Jr (1997) Pattern of interictal hypometabolism in PET scans with fludeoxyglucose F 18 reflects prior seizure types in patients with mesial temporal lobe seizures. Arch Neurol 54:129–136
15. Chassoux F et al (2004) Metabolic changes and electro-clinical patterns in mesio-temporal lobe epilepsy: a correlative study. Brain 127:164–174
16. Bartolomei F et al (1999) Seizures of temporal lobe epilepsy: identification of subtypes by coherence analysis using stereo-electro-encephalography. Clin Neurophysiol 110:1741–1754

17. Bouilleret V, Dupont S, Spelle L, Baulac M, Samson Y, Semah F (2002) Insular cortex involvement in mesio-temporal lobe epilepsy: a positron emission tomography study. Ann Neurol 51:202–208
18. Isnard J, Guenot M, Ostrowsky K, Sindou M, Mauguiere F (2000) The role of the insular cortex in temporal lobe epilepsy. Ann Neurol 48:614–623
19. Dejerine J (1895) Anatomie des centres nerveux. Rueff et Cie, Paris
20. Cointepas Y, Mangin JF, Garnero L, Poline JB, Benali H (2001) BrainVISA: Software platform for visualization and analysis of multi-modality brain data. 7th HBM 2001 Brighton, UK
21. Mangin JF, Poupon C, Clark C, Le Bihan D, Bloch I (2002) Distortion correction and robust tensor estimation for MR diffusion imaging. Med Image Anal 6:191–198
22. Pajevic S, Pierpaoli C (1999) Color schemes to represent the orientation of anisotropic tissues from diffusion tensor data: application to white matter fiber tract mapping in the human brain. Magn Reson Med 42:526–540
23. Conturo TE et al (1999) Tracking neuronal fiber pathways in the living human brain. Proc Natl Acad Sci USA 96:10422–10427
24. Kier EL, Staib LH, Davis LM, Bronen RA (2004) MR imaging of the temporal stem: anatomic dissection tractography of the uncinate fasciculus, inferior occipitofrontal fasciculus, and Meyer's loop of the optic radiation. AJNR Am J Neuroradiol 25:677–691
25. Mori S, Crain BJ, Chacko VP, van Zijl PC (1999) Three-dimensional tracking of axonal projections in the brain by magnetic resonance imaging. Ann Neurol 45:265–269
26. Team RDC (2006) R: a language and environment for statistical computing. Vienna
27. Kubicki M et al (2002) Uncinate fasciculus findings in schizophrenia: a magnetic resonance diffusion tensor imaging study. Am J Psychiatr 159:813–820
28. Park HJ et al (2004) White matter hemisphere asymmetries in healthy subjects and in schizophrenia: a diffusion tensor MRI study. Neuroimage 23:213–223
29. Highley JR, Walker MA, Esiri MM, Crow TJ, Harrison PJ (2002) Asymmetry of the uncinate fasciculus: a post-mortem study of normal subjects and patients with schizophrenia. Cereb Cortex 12:1218–1224
30. Westerhausen R, Walter C, Kreuder F, Wittling RA, Schweiger E, Wittling W (2003) The influence of handedness and gender on the microstructure of the human corpus callosum: a diffusion-tensor magnetic resonance imaging study. Neurosci Lett 351:99–102
31. Beaulieu C (2002) The basis of anisotropic water diffusion in the nervous system - a technical review. NMR Biomed 15:435–455
32. Bhagat YA, Beaulieu C (2004) Diffusion anisotropy in subcortical white matter and cortical gray matter: changes with aging and the role of CSF-suppression. J Magn Reson Imaging 20:216–227
33. Pfefferbaum A, Sullivan EV, Hedehus M, Lim KO, Adalsteinsson E, Moseley M (2000) Age-related decline in brain white matter anisotropy measured with spatially corrected echo-planar diffusion tensor imaging. Magn Reson Med 44:259–268
34. Eriksson SH, Rugg-Gunn FJ, Symms MR, Barker GJ, Duncan JS (2001) Diffusion tensor imaging in patients with epilepsy and malformations of cortical development. Brain 124:617–626
35. Concha L, Beaulieu C, Gross DW (2005) Bilateral limbic diffusion abnormalities in unilateral temporal lobe epilepsy. Ann Neurol 57:188–196
36. Babb TL, Brown MJ (1987) Pathological findings in epilepsy. In: Engel J Jr (ed) Surgical treatment of the epilepsies. Raven, New York, pp 511–540
37. Margerison JH, Corsellis JA (1966) Epilepsy and the temporal lobes. A clinical, electroencephalographic and neuropathological study of the brain in epilepsy, with particular reference to the temporal lobes. Brain 89:499–530
38. Jones DK, Symms MR, Cercignani M, Howard RJ (2005) The effect of filter size on VBM analyses of DT-MRI data. Neuroimage 26:546–554
39. Kasper BS, Stefan H, Paulus W (2003) Microdysgenesis in mesial temporal lobe epilepsy: a clinicopathological study. Ann Neurol 54:501–506
40. Mitchell LA et al (1999) Anterior temporal abnormality in temporal lobe epilepsy: a quantitative MRI and histopathologic study. Neurology 52:327–336
41. Wieser R, Engel J Jr (1993) Surgically remediable temporal lobe syndromes. In: Engel J Jr (ed) Surgical treatment of the epilepsies. Raven, New York, pp 49–63